

Predictor-Based Compensators for Networked Control Systems with Stochastic Delays and Sampling Intervals

Matheus Wagner , Marcelo M. Morato , Antônio Augusto Fröhlich , Julio E. Normey-Rico

Abstract—The stochastic nature of time delays and sampling intervals in Networked Control Systems poses significant challenges for controller synthesis and analysis, often leading to conservative designs and degraded performance. This work presents a modeling approach for Linear Multiple-Input Multiple-Output Networked Control Systems and introduces a compensation scheme based on the Filtered Smith Predictor to mitigate the adverse effects of stochastic time delays on closed-loop performance. The proposed scheme is evaluated through numerical simulations of a well-established Cooperative Adaptive Cruise Control system. Results demonstrate that the compensator achieves near-ideal average closed-loop performance and significantly reduces response variability compared to a traditional Filtered Smith Predictor. Notably, it yields a 45% reduction in worst-case tracking error signal energy relative to an ideal baseline system with no time delays and constant sampling intervals.

Index Terms—Networked Control Systems, Predictive Control, Time-Varying Delays, Stochastic Delay, Smith Predictor.

I. INTRODUCTION

Networked Control Systems (NCS) consist of spatially distributed components connected via communication networks [1], offering interoperability across heterogeneous devices and meeting the growing computational demands of modern control systems [2].

However, NCS introduce challenges in controller analysis and design. Traditional digital control assumes fixed sampling and actuation intervals with constant time delays [3], whereas networks with shared communication media and modern processors often lead to variable, stochastic delays and sampling intervals [4].

To address these issues, various modeling and design approaches have been proposed that account for the stochastic nature of delays, either as random multiples of a fixed sampling interval [5]–[9] or as continuous random variables [10]–[12]. While discrete models require added delays and may degrade performance, continuous-delay models reduce conservatism but are typically limited to delays shorter than the sampling period [13], [14].

Matheus Wagner is with the Software/Hardware Integration Lab, Federal University of Santa Catarina, Florianópolis, Brazil

Marcelo M. Morato is with the Automation and Systems Department, Federal University of Santa Catarina, Florianópolis, Brazil and the Univ. Grenoble Alpes, CNRS, Grenoble INP (Institute of Engineering Univ. Grenoble Alpes), GIPSA-lab, 38000 Grenoble, France

Antônio Augusto Fröhlich is with the Software/Hardware Integration Lab, Federal University of Santa Catarina, Florianópolis, Brazil

Julio E. Normey-Rico is with the Automation and Systems Department, Federal University of Santa Catarina, Florianópolis, Brazil

Among the many design strategies [7], [8], [11], [12], [14]–[16], predictor-based compensators, particularly the Smith Predictor (SP) and its variants, stand out for their effectiveness in mitigating delay-induced performance loss [6], [17]–[20].

Recent SP adaptations for stochastic NCS [6], [17]–[19], [21]–[24] either approximate delays as fixed constants [6], [17], [22] or use delay measurements to adjust predictions [18], [19], [23]. Yet, fixed-delay models may not capture true system behavior, while measurement-based schemes cannot anticipate post-actuation delays—both leading to conservative designs to ensure robustness.

Given the necessity for design and analysis procedures that take into account the stochastic nature of NCS, this work proposes a modeling procedure and a time delay compensation approach for NCS, whose temporal properties are modeled as continuous random variables. Accordingly, our **main contributions** are:

- 1) A new modeling procedure is proposed for linear Multiple-Input Multiple-Output (MIMO) NCS in which time delays, sampling intervals and actuation intervals are modeled as continuous random variables, without the restriction for time delays to be smaller than the sampling intervals.
- 2) A controller design procedure employing a stochastic time delay compensator based on the Filtered Smith Predictor (FSP) architecture, along with the stability conditions for the resulting closed-loop system and numerical simulations for validation of the proposed approach.

Paper Organization. Sec. II describes the proposed NCS modeling procedure. Sec. III describes the proposed compensator design procedure based on the FSP. Sec. IV presents the stability test for the closed-loop system with the compensator presented in Sec. III. Sec. V provides a numerical example for the presented modeling and controller design procedures. Finally, Sec. VI presents the concluding remarks of this work.

II. PRELIMINARIES

Considering a Linear Time-Invariant (LTI) plant, this section presents a NCS model taking into account that the sampling instant sequence may not be strictly periodic, but corrupted with sensing jitter, and that the random delays experienced by different state variables may not be equal. Sec. II-A describes the characterization of sensing, controller and actuation instant sequences in NCS, while Sec. II-B describes the procedure to

transform the continuous-time representation of a dynamical system into a stochastic discrete-time representation for the NCS. Finally, Sec. II-C presents the procedure to obtain a state-space representation of stochastic time delays.

A. Temporal behavior of NCS

The implementation of an NCS relies on a distributed real-time task set, primarily composed of sensing, control computation, and actuation tasks that communicate over a network. Sensing tasks acquire sensor measurements, the control task computes control signals based on these measurements, and actuation tasks apply the signals to the plant via actuators. Each task generates timed events that are crucial for analyzing the closed-loop system behavior, as detailed in the following paragraphs.

The sequence of measurement events is an ordered sequence of instants in which the signals from each one of the sensors are sampled, formally defined as:

Definition II.1 (Sensing sequence). The sensing sequence for the i -th sensor in a control system, denoted by $\{t_k^i\}_{k=0}^{\infty}$, is the sequence of time instants in which a measurement is acquired by sampling the signal produced by the sensor ¹.

Sensing would ideally be performed periodically, but, in practice, the sequence of sampling instants may contain some form of uncertainty. This uncertainty is referred to as sensing jitter and is defined as:

Definition II.2 (Sensing jitter). Given a sampling period T^s , the expected sensing sequence for the i -th sensor in a control system is given by $t_k^{i,expected} := kT^s$ and the sensing jitter, denoted by $\delta t_k^{s,i}$, is defined as $\delta t_k^{s,i} := t_k^{i,expected} - t_k^i$.

The fact that sensing sequences from different sensors may not be synchronized is captured as a constant offset for the i -th sensing sequence denoted by o^i . Given the aforementioned properties, the sensing sequence for the i -th sensor in a NCS is described as:

$$t_k^i := o^i + kT^s + \delta_k^{s,i}. \quad (1)$$

A precondition for the start of the computation of the k -th control signal is that the k -th messages $m_k^{s,i}$ containing the measurements acquired at the k -th sensing sequence instants are available for the controller to consume. Those messages, though, are subject to computational and communication delays, defined as:

Definition II.3 (Sensing delay). The k -th sensing delay associated with the i -th sensor in a NCS, denoted by $D_k^{s,i}$, is the time interval between the k -th element of the sensing sequence, denoted by t_k^i , and the instant in which a message containing the acquired measurement is produced and sent to the controller.

Definition II.4 (Sensing message delay). The k -th sensing message delay associated with the i -th sensor in a NCS,

denoted by $D_k^{s,c,i}$, is the time interval between the instant in which the message containing the acquired measurement is sent and the instant in which the message is available for consumption by the controller.

Once the measurements are available for the controller task, the computation of the control signal implies an additional time delay defined as:

Definition II.5 (Control signal computation delay). The delay in the computation of the k -th control signal, denoted by D_k^c , is the time interval between the instant in which the last among the k -th messages $m_k^{s,i}$ containing the measurements of each sensor becomes available for consumption by the controller and the instant in which a set of messages is produced containing the different components of the control signal.

Furthermore, each message $m_k^{a,j}$ produced by the controller task is sent to the corresponding actuator, resulting in computational and communication delays defined as follows:

Definition II.6 (Actuation message delay). The k -th actuation message delay associated with the j -th actuator in a NCS, denoted by $D_k^{c,a,j}$, is the time interval between the instant in which the control signal computation finishes and the instant in which the corresponding actuation message is available for consumption by the actuator.

Definition II.7 (Actuation delay). The k -th actuation delay for the j -th actuator, denoted by $D_k^{a,j}$, is the time interval between the instant in which the message m_k^j containing the j -th component of the control signal is available for consumption and the instant in which the actuation command is issued to the actuator.

Finally, the sequence of actuation events is the ordered sequence of instants in which each component of the control signal is applied to the plant, formally defined as:

Definition II.8 (Actuation sequence). The actuation sequence for the j -th actuator in a control system, denoted by $\{a_k^j\}_{k=0}^{\infty}$, is the sequence of time instants in which a component of the control signal is applied to the plant through the actuator.

The definition of the actuation sequence for the j -th actuator follows directly from the instants in which the command associated with the j -th component of the control signal is issued to the respective actuator; hence, such a sequence can be defined as:

$$a_k^j := \max_i \{o^i + kT^s + \delta_k^{s,i} + D_k^{s,i} + D_k^{s,c,i}\} + D_k^c + D_k^{c,a,j} + D_k^{a,j}. \quad (2)$$

The actuation sequence is of major importance for modeling the dynamic behavior of a NCS, as it encapsulates the effects of every component of the end-to-end time delay, from measurement acquisition to the issuance of commands to the actuator, defined as follows:

Definition II.9 (Time delay). The time delay D_k^i in a control system is defined by the time interval between the acquisition of a measurement and the first application of a control signal component to the plant, such that $D_k^i = \min_j \{a_k^j\} - t_k^i$.

¹the notation $\{x_k\}_{k=0}^{\infty}$ stands for a sequence of elements x_1, x_2, \dots indexed by the variable k , assuming integer values from zero to infinity

Along with the described model for the temporal behavior of the NCS, the following specifications are assumed to be fulfilled:

- 1) The sensing sequences t_k^i must be strictly monotonically increasing, hence $t_k^i - t_{k-1}^i > 0$.
- 2) The sequences t_k^i must be loosely synchronized, meaning that given $t_k = \min_i \{t_k^i\}$ and $t_{k+1} = \min_i \{t_{k+1}^i\}$, then $t_k \leq t_k^i < t_{k+1}$ for all k .
- 3) The sequence of instants in which the control signal computation starts must be strictly monotonically increasing, hence $c_k - c_{k-1} > 0$.
- 4) The actuation sequences a_k^j must be strictly monotonically increasing, hence $a_k^j - a_{k-1}^j > 0$.
- 5) The actuation sequences a_k^j must be loosely synchronized, meaning that given $a_k = \min_j \{a_k^j\}$ and $a_{k+1} = \min_j \{a_{k+1}^j\}$, then $a_k \leq a_k^j < a_{k+1}$ for all k .

The set of specifications proposed above is considered in order to simplify the analytical treatment of the model, but is also motivated by practical considerations. Specifications (1), (3) and (4) ensure that the ordering of control signal computation and actuation events matches the ordering of sampling events. Specifications (2) and (5) enforce that every control signal computed based on the measurements from the k -th set of sensing jobs is applied to the plant before any of the components of the next control signal are applied to the plant by the next set of actuation jobs. In both cases, the fulfillment of the specifications implies an emulation of the system behavior that would be observed if all tasks were executed sequentially in a single computing device.

B. Discretization of LTI system dynamics

Consider a continuous-time LTI system described in state-space form by a set of ordinary differential equations, in which N_a is the number of actuators of the system:

$$\dot{\mathbf{x}}(t) = A^o \mathbf{x}(t) + \sum_{j=1}^{N_a} \mathbf{b}^{o,j} u^j(t). \quad (3)$$

The exact solution for the system of differential equations from Eq. (3) between two consecutive instants of the sequence $a_k = \min_j \{a_k^j\}$ is given by Eq. (4), in which $\Delta a_{k+1} = a_{k+1} - a_k$.

$$\begin{aligned} \mathbf{x}(a_{k+1}) &= e^{A^o \Delta a_{k+1}} \mathbf{x}(a_k) \\ &+ \sum_{j=1}^{N_a} \left[\int_{a_k}^{a_{k+1}} e^{A^o(a_{k+1}-\tau)} \mathbf{b}^{o,j} u^j(a_k) d\tau \right. \\ &\left. - \int_{a_k}^{a_k^j} e^{A^o(a_{k+1}-\tau)} \mathbf{b}^{o,j} (u^j(a_k) - u^j(a_{k-1})) d\tau \right]. \end{aligned} \quad (4)$$

Eq. (4) can be written in the compact form presented in Eq. (5), in which $B_k = \text{col}(\beta_k^i)$, $B_k^J = \text{col}(\beta_k^{J,j})$ and A_k are defined as $A_k = e^{A^o \Delta a_{k+1}}$. Furthermore $\mathbf{x}(a_k)$ is replaced by \mathbf{x}_k for a simpler notation, and the symbol $\Delta \mathbf{u}_k = \mathbf{u}_k - \mathbf{u}_{k-1}$ is introduced.

$$\begin{aligned} \mathbf{x}_{k+1} &= A_k \mathbf{x}_k + B_k \mathbf{u}_k + B_k^J \Delta \mathbf{u}_k. \\ \beta_k^j &= \int_{a_k}^{a_{k+1}} e^{A^o(a_{k+1}-\tau)} \mathbf{b}^{o,j} d\tau. \\ \beta_k^{J,j} &= - \int_{a_k}^{a_k^j} e^{A^o(a_{k+1}-\tau)} \mathbf{b}^{o,j} d\tau. \end{aligned} \quad (5)$$

Next, in order to obtain a proper state-space NCS model, the models representing the actuation jitter, J^u , and the dynamics of the plant, G , presented in equations (6) and (7), respectively, must be arranged in a series connection, leading to the model of the system in the absence of time delays. The term $B_k^w \mathbf{w}_k$ is included in the system defined by Eq. (7) to represent possible exogenous disturbances.

$$J^u : \begin{cases} \mathbf{x}_{k+1}^{J^u} = \mathbf{u}_k \\ \mathbf{u}_k^{J^u} = -B_k^J \mathbf{x}_k^{J^u} + (B_k + B_k^J) \mathbf{u}_k. \end{cases} \quad (6)$$

$$G : \begin{cases} \mathbf{x}_{k+1} = A_k \mathbf{x}_k + \mathbf{u}_k^{J^u} + B_k^w \mathbf{w}_k \\ \mathbf{y}_k = \mathbf{x}_k. \end{cases} \quad (7)$$

C. Stochastic delays

For deterministic digital control systems, time delays can be incorporated into state-space models as a minimal realization of the z^{-d} transfer function, having d as a time delay expressed as a multiple of the sampling period. Next, we derive an extension of such a model that accounts for time delays represented by a continuous random variable.

Next, in order to obtain a state-space representation of stochastic time delays, we first denote a given time delay observation as D_k^i , which is decomposed into an integer and a fractional part - $N_k^{i,d}$ and d_k^i , respectively. The latter are, by construction, stochastic variables and defined as follows:

$$N_k^{i,d} := \{n > 1; a_{k-n} \leq a_k - D_k^i < a_{k-n+1}\}. \quad (8)$$

$$d_k^i := \sum_{n=1}^{N_k^{i,d}} \Delta a_{k-n+1} - D_k^i. \quad (9)$$

Note that the fractional part of the delay in Eq. (9) is expressed as a time-advancement, as it will be more convenient for the modeling steps presented later in this Section.

To determine a proper state-space model to represent the stochastic time delay operator, it is necessary to relate the i -th component of $\mathbf{x}(a_{k-N_k^{i,d}} + d_k^i)$ to $\mathbf{x}(a_{k-N_k^{i,d}})$, modeling the fractional part of the delay, and then relate $\mathbf{x}(a_{k-N_k^{i,d}})$ to $\mathbf{x}(a_k)$, modeling the integer part of the delay.

The model for the fractional part of the delay is based on the exact solution of Eq. (3) considering two different scenarios for each component of the control signal, one in which $a_{k-N_k^{i,d}} + d_k^i \in [a_{k-N_k^{i,d}}, a_{k-N_k^{i,d}}^j]$ and another in which $a_{k-N_k^{i,d}} + d_k^i \in [a_{k-N_k^{i,d}}^j, a_{k-N_k^{i,d}+1}]$. Both scenarios are captured in Eqs. (10)-(12), in which the random variable $p_k^{i,j}$ equals 1 if $a_{k-N_k^{i,d}} + d_k^i \in [a_{k-N_k^{i,d}}, a_{k-N_k^{i,d}}^j]$ and zero otherwise, $\Gamma_k^{i-} = \text{col}(\Gamma_k^{i,j-})$ and $\Gamma_k^{i+} = \text{col}(\Gamma_k^{i,j+})$.

$$\mathbf{x}(a_{k-N_k^{i,d}} + d_k^i) = e^{A^o d_k^i} \mathbf{x}(a_{k-N_k^{i,d}}) + \Gamma_k^{i-} \mathbf{u}(a_{k-N_k^{i,d}-1}) + \Gamma_k^{i+} \mathbf{u}(a_{k-N_k^{i,d}}). \quad (10)$$

$$\Gamma_k^{ij-} = p_k^{ij} \int_{a_{k-N_k^{i,d}}}^{a_{k-N_k^{i,d}} + d_k^i} e^{A^o(a_{k-N_k^{i,d}} + d_k^i - \tau)} \mathbf{b}^{o,j} d\tau + (1 - p_k^{ij}) \int_{a_{k-N_k^{i,d}}}^{a_{k-N_k^{i,d}} + s_{k-N_k^{i,d}}^j} e^{A^o(a_{k-N_k^{i,d}} + d_k^i - \tau)} \mathbf{b}^{o,j} d\tau. \quad (11)$$

$$\Gamma_k^{ij+} = (1 - p_k^{ij}) \int_{a_{k-N_k^{i,d}}}^{a_{k-N_k^{i,d}} + d_k^i} e^{A^o(a_{k-N_k^{i,d}} + d_k^i - \tau)} \mathbf{b}^{o,j} d\tau. \quad (12)$$

The model for the integer time delays, defined in Eq. (13), relies on the fact that there exists N_{\max}^d such that $N_k^{i,d} \leq N_{\max}^d$ for all $k > 0$, since the probability distributions of all components of the time delays are assumed to have compact support.

$$\mathbf{x}_{k+1}^l = A^l \mathbf{x}_k^l + B^d \mathbf{u}_k^l. \quad (13)$$

$$A^l = \begin{bmatrix} \mathbf{0}_{1 \times N_{\max}^d - 1} & \mathbf{0}_{1 \times 1} \\ \mathbf{I}_{N_{\max}^d - 1 \times N_{\max}^d - 1} & \mathbf{0}_{N_{\max}^d - 1 \times 1} \end{bmatrix}, B^l = \begin{bmatrix} 1 \\ \mathbf{0}_{N_{\max}^d - 1 \times 1} \end{bmatrix}.$$

Given an admissible initial condition, the state vector of the system described by Eq. (13) contains the delayed observations of a scalar input u_k^l up to $u_{k-N_{\max}^d}^l$. For a given delay observation $N_k^{i,d}$, the corresponding delayed input $u_{k-N_k^{i,d}}^l$ can be recovered by selecting a matrix $C^{l, N_k^{i,d}}$ such that the equality $C^{l, N_k^{i,d}} \mathbf{x}_k^l = u_{k-N_k^{i,d}}^l$ is satisfied. This same rationale can be extended for vector inputs by simply considering the parallel composition of multiple instances of the system described by Eq. (13).

The dynamics of the term $e^{A^o d_k^i} \mathbf{x}(a_{k-N_k^{i,d}})$ from Eq. (10) is captured by the system described in Eq. (14), considering the input of the system to be $\mathbf{u}_k^{lx} = \mathbf{x}(a_k) = \mathbf{x}_k$. The matrices A^{lx} and B^{lx} are given by the dynamic and input matrices of the parallel composition of the system described by Eq. (13), respectively. The output matrix C^{lx} is a stochastic matrix given by $C^{lx} = e^{A^o d_k^i} C^{lx, N_k^{i,d}}$, with $C^{lx, N_k^{i,d}}$ being the stochastic output matrix of the integer delay system.

$$L^x : \begin{cases} \mathbf{x}_{k+1}^{lx} = A^{lx} \mathbf{x}_k^{lx} + B^{lx} \mathbf{u}_k^{lx} \\ \mathbf{y}_k^{lx} = C_k^{lx} \mathbf{x}_k^{lx}. \end{cases} \quad (14)$$

The same rationale can be applied to obtain the dynamics of the terms from Eq. (10) related to $\mathbf{u}(a_{k-N_k^{i,d}-1})$ and $\mathbf{u}(a_{k-N_k^{i,d}})$, which generates:

$$L^u : \begin{cases} \mathbf{x}_{k+1}^{lu} = A^{lx} \mathbf{x}_k^{lu} + B^{lu} \mathbf{u}_k^{lu} \\ \mathbf{y}_k^{lu} = C_k^{lx} \mathbf{x}_k^{lu}. \end{cases} \quad (15)$$

By combining the control signal and state delay models presented, it is possible to define the undisturbed dynamics of a closed-loop system based solely on the state vector \mathbf{x}_k ,

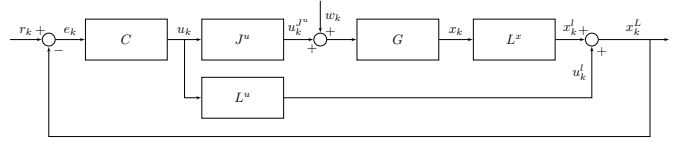


Fig. 1. Closed loop system with fractional and integer time delays

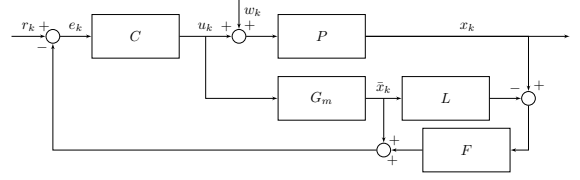


Fig. 2. Filtered Smith predictor structure

the input vector \mathbf{u}_k and their integer delayed values, while considering the stochastic nature of time delays. A block diagram of the resulting system representation is presented in Fig. 1.

III. COMPENSATOR DESIGN

Sec. II introduces the notation and provides an overview of the proposed model for NCS. This section presents the main contribution of this work: a design method for time-delay compensators for NCS described by the proposed model.

The original FSP was designed to compensate for the effects of constant time delays in a closed-loop control system by using a predictor of the non-delayed outputs of the plant [25]. It is composed of a primary controller C , designed to stabilize the delay-free model of a LTI plant G_m , the actual plant P , including time delays, a model for the plant time delay L and the prediction error filter F organized in the topology presented in Fig. 2.

The feedback signal \bar{x}_k supplied to the controller is given by the delay-free plant model, hence the system is able to anticipate the response of the time delay system and effectively track the reference signals as if there were no time delays. In reality, modeling errors and external disturbances are unavoidable. For this reason, the prediction error is used along with the delay-free model prediction to produce a more accurate estimate of the delay-free outputs. The role of the prediction error filter is to grant greater robustness to the overall system in exchange for slower response to disturbances. The procedure outlined in this section aims at deriving a variation of the FSP that considers the state-space stochastic model for NCS proposed in the previous sections, referred to as the Stochastic State-Space Filtered Smith Predictor (3SFSP).

The systematic design process of a FSP consists of three parts. First, the primary controller is designed using any available technique, considering the delay-free model of the plant. Secondly, a model of the plant including time delays is established in order to build the predictor. Finally, the prediction error filter is tuned to meet a robustness specification and to avoid the appearance of undesired plant model poles in the predictor dynamics, yielding a stable predictor even for unstable plant models.

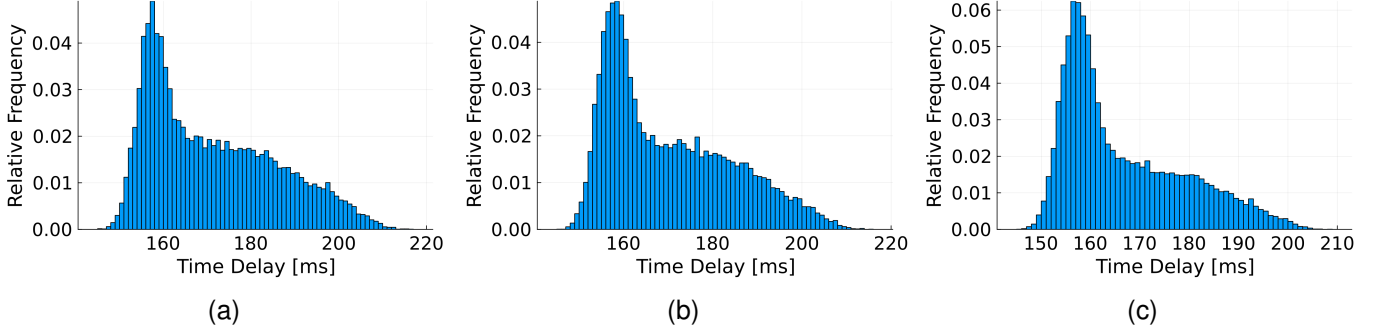


Fig. 5. Time delay histograms for the numerical example. (a) Time delay observations for x^1 . (b) Time delay observations for x^2 . (c) Time delay observations for x^3 .

- 2) Compute the Monte-Carlo estimation of $E\{A_k^{aT} \otimes A_k^{aT}\}$ using the samples acquired in step 1.
- 3) Compute the eigenvalues of $E\{A_k^{aT} \otimes A_k^{aT}\}$ and assert that the associated spectral radius is smaller than one.

V. NUMERICAL EXAMPLE

In order to demonstrate the effectiveness of the proposed approach, this section presents a numerical example considering the Cooperative Adaptive Cruise Control System (CACCS) from Ploeg et al. [27], commonly employed to evaluate NCS design strategies [28], [29].

The objective of the CACCS is to control the distance between vehicles, considering a time headway, through the cooperation of the vehicles in a platoon. For simplicity, this work considers only two vehicles for the numerical example.

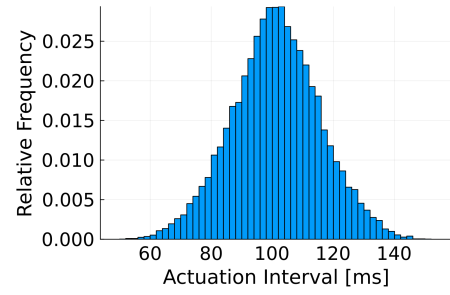
The continuous-time state-space model for the CACCS is given by Eq. (23) and Eq. (24), in which τ^{-1} is a parameter of the engine dynamics and h is the time headway. The components of $\mathbf{x} = [x_1, x_2, x_3]$ represent the spacing, velocity, and acceleration differences between two vehicles, respectively, while the components of $\mathbf{u} = [u_1, u_2]$ represent the acceleration commands from the follower and the leader vehicles, respectively.

$$\dot{\mathbf{x}} = A^x \mathbf{x} + B^x \mathbf{u} + B^w \mathbf{w}. \quad (23)$$

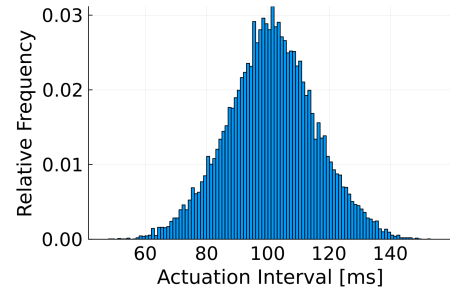
$$A^x = \begin{bmatrix} 0 & 1 & 0 \\ 0 & 0 & 1 \\ 0 & 0 & -\tau^{-1} \end{bmatrix}, \quad (24)$$

$$B^x = \begin{bmatrix} 0 & 0 \\ 0 & 0 \\ h\tau^{-1} & -\tau^{-1} \end{bmatrix}, \quad B^w = \begin{bmatrix} 0 & 0 \\ 0 & 0 \\ 1 & 1 \end{bmatrix}.$$

For controller design, the continuous-time sis exactly discretized, considering a sampling period $T_s = 100$ ms. The primary controller structure consists of a dynamic controller, to include integral action, and a state-feedback gain designed using the discrete LQR procedure, resulting in the controller described in Eqs. (25) and (26), in which r_k is the inter-vehicle spacing reference to be tracked, hence $\mathbf{B}^r = [1, 0, 0]^T$. The matrices employed in the cost function for the LQR design were $Q = 2I/3$ and $R = I/3$.



(a)



(b)

Fig. 6. Actuation interval histograms for the numerical example. (a) Actuation interval observations for u^1 . (b) Actuation interval observations for u^2 .

$$\begin{cases} \mathbf{x}^c_{k+1} = A^c \mathbf{x}^c_k + B^c (\mathbf{B}^r r_k - \mathbf{x}_k) \\ \mathbf{u}_k = -K^c \mathbf{x}^c_k + K^x (\mathbf{B}^r r_k - \mathbf{x}_k). \end{cases} \quad (25)$$

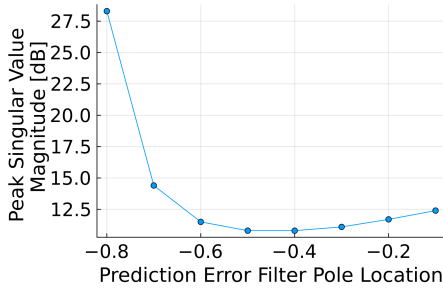
$$A^c = 1, \quad B^c = \begin{bmatrix} 1 \\ 0 \\ 0 \end{bmatrix}, \quad K^c = \begin{bmatrix} 0.5986 \\ -0.8551 \end{bmatrix} \quad (26)$$

$$K^x = \begin{bmatrix} -7.8336 & -4.7042 & -1.1818 \\ 11.1908 & 6.7202 & 1.6883 \end{bmatrix}.$$

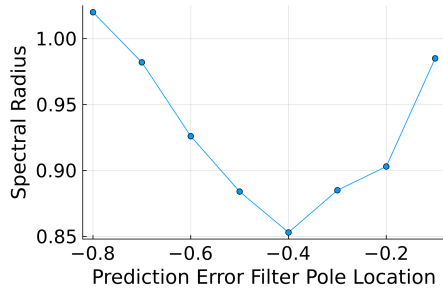
The probability distributions for the temporal properties of the NCS are presented in Table I. The Inverse Gaussian distribution was selected to characterize the execution time of tasks and transmission time of messages as previous works in the literature have pointed to it as a good fit for modeling

TABLE I
NCS PROBABILITY DISTRIBUTION PARAMETERS FOR THE EXAMPLE

System Property	Distribution and Parameters
Sensing Offset	Uniform (min=0s, max=20ms)
Sensing Jitter	Uniform (min=0s, max=50ms)
Sensing Task Delay	Truncated Inverse Gaussian ($min = 14ms$, $max = 17ms$, $\mu = 16ms$, $\sigma = 0.85ms$)
Sensing Message Delay	Truncated Inverse Gaussian ($min = 28ms$, $max = 34ms$, $\mu = 32ms$, $\sigma = 1.7ms$)
Control Computation Delay	Truncated Inverse Gaussian ($min = 42ms$, $max = 51ms$, $\mu = 48ms$, $\sigma = 2.5ms$)
Actuation Message Delay	Truncated Inverse Gaussian ($min = 42ms$, $max = 51ms$, $\mu = 48ms$, $\sigma = 2.5ms$)
Actuation Task Delay	Truncated Inverse Gaussian ($min = 14ms$, $max = 17ms$, $\mu = 16ms$, $\sigma = 0.85ms$)



(a)



(b)

Fig. 7. Parametric analysis for selection of the prediction filter pole location. (a) Peak of the singular value frequency response from the input disturbance to output transfer function. (b) Spectral radius of the matrix $\Xi^T \otimes \Xi$.

response times [30]. The truncated Inverse Gaussian distribution is a variation of the regular Inverse Gaussian distribution that has compact support. Fig. 5 and Fig. 6 present the histograms of the resulting time delay and actuation interval observations. Given the probability distributions for the NCS temporal properties, the primary controller and the continuous-time model of the plant, the discrete-time stochastic models for the plant, input jitter and time delays were obtained using the procedure outlined in Sec. II.

The filter design is carried out considering the diagonal filter structure from Eq. (27). The zeros of the filter are designed to prevent the plant poles at $z = -1$, as well as the pole of the

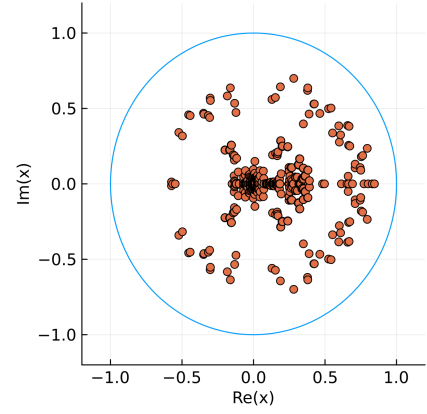


Fig. 8. Pole diagram related to $E\{A_k^{aT} \otimes A_k^{aT}\}$ for the system of the numerical example.

plant at $z = -0.819$, of appearing in the predictor dynamics. The poles of the filter are chosen based on a parametric analysis considering the spectral radius of the matrix $\Xi^T \otimes \Xi$, which is correlated with the set-point response performance, and the peak of the singular value frequency response from the expected value of the input disturbance to output transfer function, which is a metric for the robustness of the closed-loop system. As presented in Fig. 7, the parametric analysis results indicate that the best compromise between disturbance rejection and set-point responses is achieved when the pole location is given by $\alpha = 0.4$, which is the pole location selected for this design step.

$$\begin{aligned}
 F_{11}(z) &= \frac{b_{14}z^4 + b_{13}z^3 + b_{12}z^2 + b_{11}z + b_{10}}{(z - \alpha)^5} \\
 F_{22}(z) &= \frac{b_{14}z^4 + b_{13}z^3 + b_{12}z^2 + b_{11}z + b_{10}}{(z - \alpha)^5} \\
 F_{33}(z) &= \frac{b_{31}z + b_{30}}{(z - \alpha)^2}.
 \end{aligned} \tag{27}$$

The stability test of the closed-loop system is carried out through a Monte-Carlo estimation using ten thousand observations of A_k^{aT} , which was shown to be enough for the convergence of the estimate. The resulting eigenvalues of $E\{A_k^{aT} \otimes A_k^{aT}\}$ are presented in Fig. 8. By inspection, it is possible to conclude that stability is ensured according to the proposed test detailed in Sec. IV, as all poles lie within the unit circle and the spectral radius of $E\{A_k^{aT} \otimes A_k^{aT}\}$ is 0.856.

Then, to verify the effectiveness of the 3SFSP, a set of numerical simulations was performed to compare the response of the system in ideal conditions, i.e. constant sampling intervals and no time delays, with the response of the system with and without the compensation scheme provided by the 3SFSP. Furthermore, a comparison with a classical FSP, referred to as the baseline compensator, considering a fixed delay of two sampling periods and a pole location for the filter at $\alpha = 0.3$ was also performed. For each case, 5000 observations of the system response were evaluated, enough for the convergence of the ensemble average of observations. Accordingly, Fig. 9 presents the response of the systems to a unit step in the

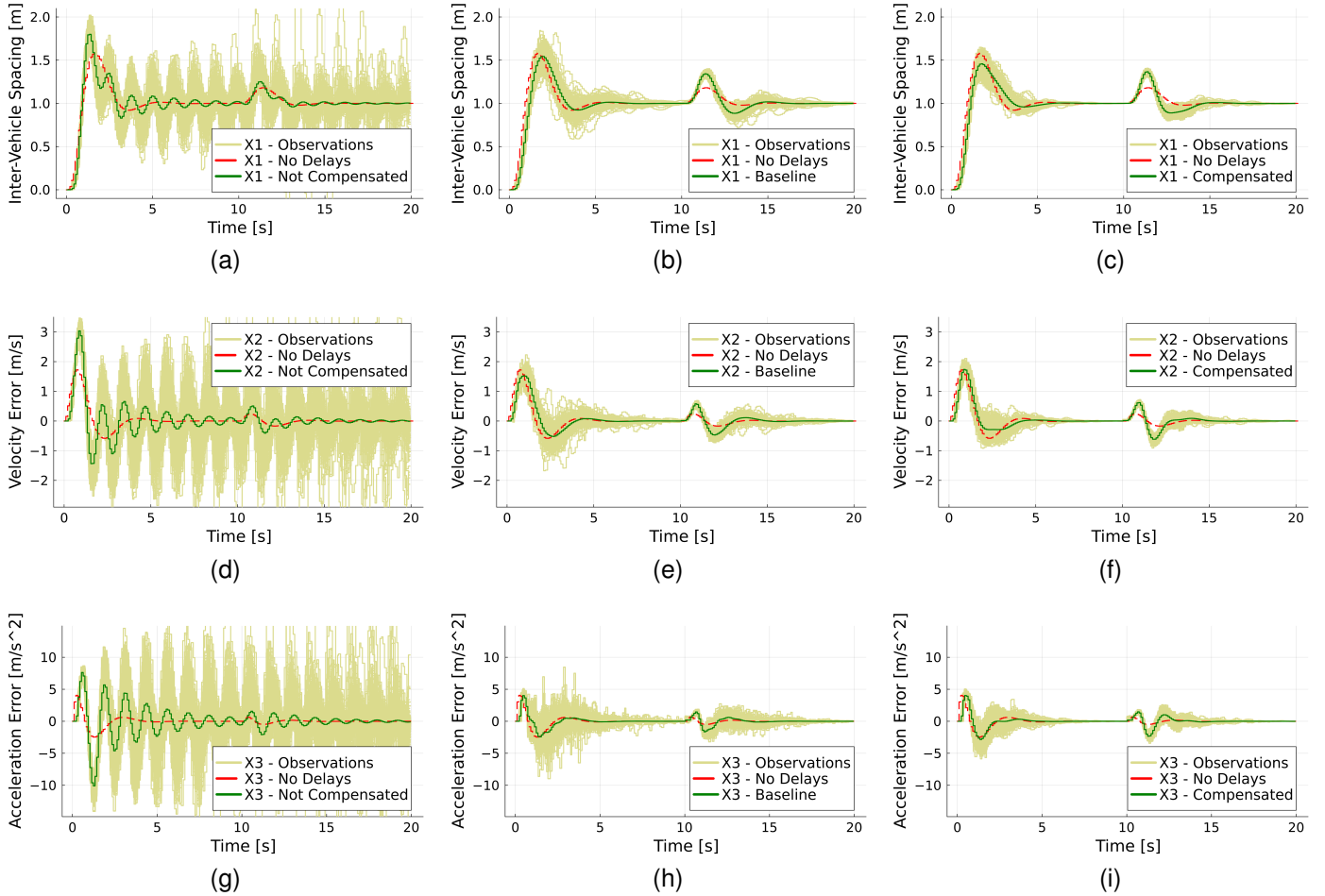


Fig. 9. Observations of the system states time response for the numerical examples. Inter-vehicle spacing (x^1) (a) in the absence of time delay compensation, (b) using the baseline time delay compensator and (c) using the 3SFSP time delay compensator. Velocity error (x^2) (d) in the absence of time delay compensation, (e) using the baseline time delay compensator and (f) using the 3SFSP time delay compensator. Acceleration error (x^3) (g) in the absence of time delay compensation, (h) using the baseline time delay compensator and (i) using the 3SFSP time delay compensator.

reference inter-vehicle distance and to a constant disturbance of magnitude $10m/s^2$ applied at the instant $t = 10s$. The corresponding control signals resulting from the simulation are presented in Fig. 10.

The results presented in Fig. 9 highlight that the oscillatory behavior induced by the time delays in the absence of compensation is completely removed once the 3SFSP or the FSP is used for compensation. Furthermore, the application of the 3SFSP reduced the overall variance observed across different observations of the system response. When compared to the classical FSP, the response of the system compensated by 3SFSP presents a reduced variance across different observations of the system response.

Although the step response ensemble average of the compensated system in Fig. 9 closely resembles the ideal step response, the response to disturbances does not. This occurs due to the fact that for the 3SFSP, like the FSP, the response to disturbances is heavily influenced by the response of the prediction error filter whose zeros are constrained by the design requirement of avoiding the appearance of undesired poles of the plant model in the predictor dynamics. But even with

the observed amplification of disturbances in the compensated scenario, the overall disturbance rejection performance of the system increases once the compensation scheme of the 3SFSP is employed.

For a quantitative evaluation of the system's performance, each observation of the system response was evaluated with respect to the metric presented in Eq. (28), that measures the energy of the tracking error signal.

$$J = \sum_{n=0}^N \|\mathbf{B}^T r_k - \mathbf{x}\|^2. \quad (28)$$

Fig. 11 presents the performance of the system relative to the performance of the system in ideal conditions, denoted by J_{ideal} , computed as the ratio J/J_{ideal} , while Fig 12 presents a performance comparison between the 3SFSP and FSP (baseline). The quantitative performance comparison clearly states the performance improvement observed through the use of the 3SFSP or the FSP. For the case in which no compensation is employed, the average and worst tracking error signal energy observed are 9.27 and 407 times that of the system in ideal conditions, respectively. For the case in which the 3SFSP is

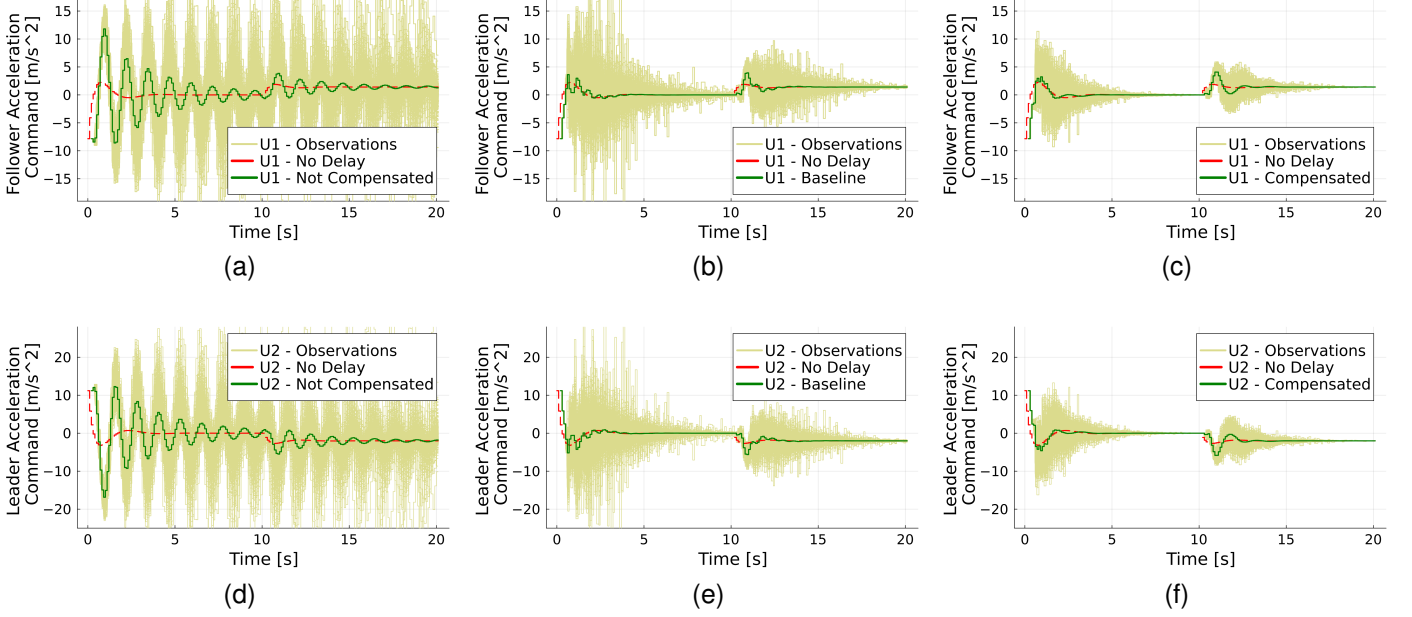


Fig. 10. Observations of the control signal time response for the numerical examples. Follower vehicle acceleration command (u^1) (a) in the absence of time delay compensation, (b) using the baseline time delay compensator and (c) using the 3SFSP time delay compensator. Leader vehicle acceleration command (u^2) (d) in the absence of time delay compensation, (e) using the baseline time delay compensator and (f) using the 3SFSP time delay compensator.

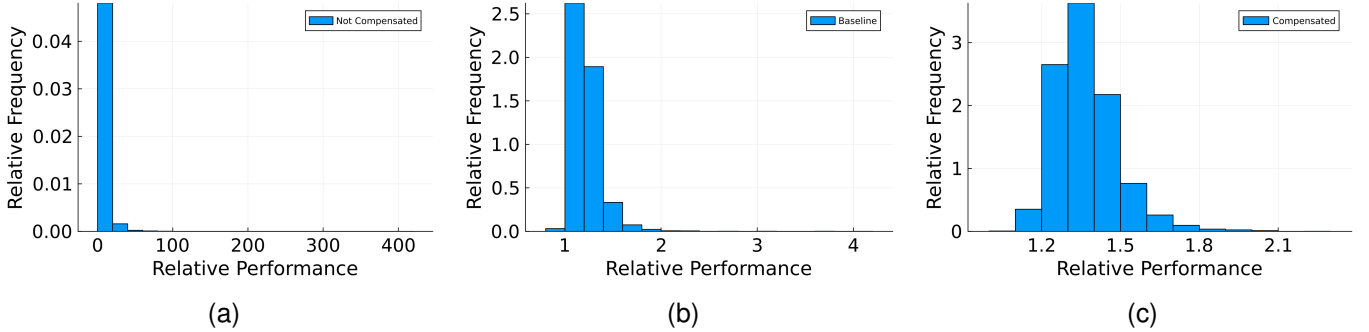


Fig. 11. Performance relative to the case with fixed sampling period and without time delays. (a) No compensation. (b) Baseline compensator. (c) 3SFSP compensator.

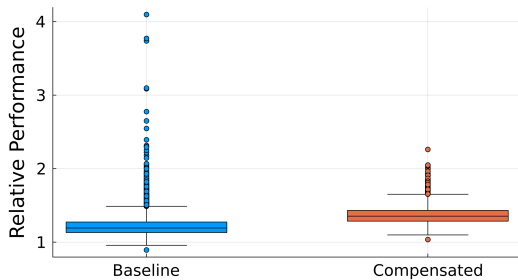


Fig. 12. Box plot for the performance relative to the case with fixed sampling period and without time delays considering the baseline and 3SFSP compensators

employed, the average and worst tracking error signal energy observed are 1.37 and 2.26 times that of the system in ideal conditions, respectively. For the case in which the FSP is

employed, the average and worst tracking error signal energy observed are 1.23 and 4.10 times that of the system in ideal conditions, respectively. The quantitative analysis confirms the qualitative observation that the 3SFSP provides a smaller variability on the system performance when compared with the FSP, demonstrating how, beyond effectively compensating stochastic time delays, the 3SFSP attenuates the uncertainty propagation from the time delays to the system response.

VI. CONCLUSION

This work presented modeling, design and analysis procedures for stochastic NCS considering a compensation scheme based on the FSP. The effectiveness of the proposed compensation scheme was evaluated through a numerical simulation considering a well-established model for a CACCS. The presented results demonstrate that by employing the 3SFSP for time delay compensation, the performance of the closed-loop

system can be made very close to that of an ideal realization of the system.

It is important to highlight that the proposed approach is applicable to LTI plants in which the full state of the system is measurable and to NCS with a very high degree of network reliability, in terms of how often messages fail to be delivered. Hence, further work is still necessary to broaden the range of systems that can benefit from the 3SFSP topology. Furthermore, in further work, we aim to relax the specifications imposed on the response times of the control system tasks by compensating violations of such specifications and investigate the representativeness of the Independent and Identically Distributed (IID) model for response time.

ACKNOWLEDGMENTS

The Authors acknowledge the financial support from *Coordenação de Aperfeiçoamento de Pessoal de Nível Superior – Brasil (CAPES)* [finance code 001 and grant 88881.878833/2023 – 01 - OPCOMPLEX, SticAmSud], from the National Council for Scientific and Technological Development (CNPq, Brazil) [grants 304032/2019-0, 403949/2021-1, and 406477/2022-1], and from FAPESC [project 2023TR001506].



**Funded by
the European Union**

This work has been funded by European Union's Horizon Europe research and innovation programme under the *Marie Skłodowska-Curie Action* grant agreement No 101149263 (*REAL OPT 4 CONTROL*).

REFERENCES

- [1] J. Baillieul and P. J. Antsaklis, "Control and communication challenges in networked real-time systems," *Proceedings of the IEEE*, vol. 95, no. 1, pp. 9–28, 2007.
- [2] J. R. Moyne and D. M. Tilbury, "The emergence of industrial control networks for manufacturing control, diagnostics, and safety data," *Proceedings of the IEEE*, vol. 95, no. 1, pp. 29–47, 2007.
- [3] G. F. Franklin, J. D. Powell, A. Emami-Naeini, and J. D. Powell, *Feedback control of dynamic systems*. Prentice hall Upper Saddle River, 2002, vol. 4.
- [4] K. Liu, A. Selivanov, and E. Fridman, "Survey on time-delay approach to networked control," *Annual Reviews in Control*, vol. 48, pp. 57–79, 2019.
- [5] Z. Pang, C. Bai, G. Liu, Q. Han, and X. Zhang, "A novel networked predictive control method for systems with random communication constraints," *Journal of Systems Science and Complexity*, vol. 34, no. 4, pp. 1364–1378, Aug 2021. [Online]. Available: <https://doi.org/10.1007/s11424-021-0160-y>
- [6] M. Steinberger and M. Horn, "Robust filtered smith predictors for networked control systems with packet-based data transmission," *Journal of Process Control*, vol. 111, pp. 86–96, 2022.
- [7] M. Bahreini and J. Zarei, "Robust finite-time fault-tolerant control for networked control systems with random delays: A markovian jump system approach," *Nonlinear Analysis: Hybrid Systems*, vol. 36, p. 100873, 2020.
- [8] P. Haghghi, B. Tavassoli, and A. Farhadi, "A practical approach to networked control design for robust \mathcal{H}_∞ performance in the presence of uncertainties in both communication and system," *Applied Mathematics and Computation*, vol. 381, p. 125308, 2020.
- [9] D. J. Antunes and H. Qu, "Frequency-domain analysis of networked control systems modeled by markov jump linear systems," *IEEE Transactions on Control of Network Systems*, vol. 8, no. 2, pp. 906–916, 2021.
- [10] Z. Hu, F. Deng, Y. Su, S. Luo, Y. Liu, and K. Chen, "Stability analysis and synthesis for networked systems with noisy sampling intervals, random transmission delays and packet dropouts," *IEEE Transactions on Automatic Control*, 2023.
- [11] Z. Hu, H. Song, H. Ren, Y. Su, and F. Deng, "Stabilization of networked control systems subject to noisy sampling intervals and stochastic time-varying delays," *IEEE Transactions on Control of Network Systems*, vol. 9, no. 3, pp. 1271–1280, 2022.
- [12] Y. Su, Z. Hu, K. Chen, T. Luo, and Y. Li, " \mathcal{H}_∞ control of networked systems with noisy sampling intervals and actuators saturation," *Int. J. Innov. Comput. Inf. Control*, vol. 18, no. 4, pp. 1317–1328, 2022.
- [13] Z. Hu, J. Zhang, F. Deng, Z. Fan, and L. Qiu, "A discretization approach to sampled-data stabilization of networked systems with successive packet losses," *International Journal of Robust and Nonlinear Control*, vol. 31, no. 10, pp. 4589–4601, 2021.
- [14] H. Sun, J. Sun, and J. Chen, "Analysis and synthesis of networked control systems with random network-induced delays and sampling intervals," *Automatica*, vol. 125, p. 109385, 2021.
- [15] P. Haghghi and B. Tavassoli, "Static output feedback control of uncertain systems over uncertain communication links with guaranteed \mathcal{H}_∞ performance," *International Journal of Robust and Nonlinear Control*, vol. 31, no. 5, pp. 1514–1529, 2021.
- [16] X. Lu, Y. Cai, H. Wang, H. Wang, G. Zhang, and X. Liang, "Necessary and sufficient condition of optimal control for networked control systems with markovian packet dropouts," *International Journal of Control, Automation and Systems*, vol. 21, no. 5, pp. 1485–1492, 2023.
- [17] S. Bonala, B. Subudhi, and S. Ghosh, "On delay robustness improvement using digital smith predictor for networked control systems," *European Journal of Control*, vol. 34, pp. 59–65, 2017.
- [18] A. P. Batista and F. G. Jota, "Performance improvement of an ncs closed over the internet with an adaptive smith predictor," *Control Engineering Practice*, vol. 71, pp. 34–43, 2018.
- [19] H. Mo and G. Sansavini, "Hidden markov model-based smith predictor for the mitigation of the impact of communication delays in wide-area power systems," *Applied Mathematical Modelling*, vol. 89, pp. 19–48, 2021.
- [20] J. E. Normey-Rico, T. L. Santos, R. C. Flesch, and B. C. Torrico, "Control of dead-time process: From the smith predictor to general multi-input multi-output dead-time compensators," *Frontiers in Control Engineering*, vol. 3, p. 953768, 2022.
- [21] M. M. Morato and J. E. Normey-Rico, "A novel unified method for time-varying dead-time compensation," *ISA transactions*, vol. 108, pp. 78–95, 2021.
- [22] M. Gamal, N. Sadek, M. R. Rizk, and A. K. Abou-elSaoud, "Delay compensation using smith predictor for wireless network control system," *Alexandria Engineering Journal*, vol. 55, no. 2, pp. 1421–1428, 2016.
- [23] A. Cuenca, J. Salt, V. Casanova, and R. Pizá, "An approach based on an adaptive multi-rate smith predictor and gain scheduling for a networked control system: implementation over profibus-dp," *International Journal of Control, Automation and Systems*, vol. 8, pp. 473–481, 2010.
- [24] Y. Wu and Y. Wu, "A novel predictive control scheme with an enhanced smith predictor for networked control system," *Automatic Control and Computer Sciences*, vol. 52, pp. 126–134, 2018.
- [25] J. Normey-Rico and E. Camacho, *Control of Dead-Time Processes*, 01 2007.
- [26] J. Nilsson, "Real-time control systems with delays," 1998.
- [27] J. Ploeg, B. T. Scheepers, E. Van Nunen, N. Van de Wouw, and H. Nijmeijer, "Design and experimental evaluation of cooperative adaptive cruise control," in *2011 14th International IEEE Conference on Intelligent Transportation Systems (ITSC)*. IEEE, 2011, pp. 260–265.
- [28] H. Saito, Y. Katsuki, A. Sawabe, Y. Shinohara, T. Iwai, and R. Kubo, "Network and control co-design for heterogeneous cacc systems under communication constraints," in *2024 IEEE International Conference on Industrial Technology (ICIT)*. IEEE, 2024, pp. 1–6.
- [29] S. E. Li, Y. Zheng, K. Li, L.-Y. Wang, and H. Zhang, "Platoon control of connected vehicles from a networked control perspective: Literature review, component modeling, and controller synthesis," *IEEE Transactions on Vehicular Technology*, 2017.
- [30] K. Zagalo, O. Verbytska, L. Cucu-Grosjean, and A. Bar-Hen, "Response times parametric estimation of real-time systems," 2022.